Materials and Structures (2007) 40:865–875
DOI 10.1617/s11527-006-9189-6

ORIGINAL ARTICLE

# Numerical simulation of the hydration process and the development of microstructure of self-compacting cement paste containing limestone as filler

**G. Ye · X. Liu · A. M. Poppe · G. De Schutter · K. van Breugel**

Received: 26 September 2005 / Accepted: 12 June 2006 / Published online: 27 January 2007


**Abstract** This paper presents a numerical model for the simulation of the hydration process and the development of the microstructure on Self-compacting cement paste (SCC) containing limestone powder as filler. Based on a series of experimental results, e.g. thermometric isothermal conduction calorimetry tests, environmental scanning electron microscopy (ESEM) image analysis, thermogravimetric analysis (TGA) and the derivative thermogravimetric analysis (DTG) measurements, the hydration process, the solid phase distribution, total porosity and pore size distribution have been determined at different hydration stages.

Based on the hydration chemistry, the stoichiometry and the hydration kinetics of cement with limestone, an analytical hydration model and a microstructural model of self-compacting cement paste are proposed. Two SCC mixtures with w/c 0.41 and w/c 0.48, both with water/powder ratio (w/p) 0.27, were simulated and compared to a traditional cement paste (TC) with w/c 0.48. The simulation results were discussed and validated against experimental measurements.

**Résumé** *Cet article présente un modèle numérique qui réalise une simulation du processus d'hydratation et le développement de la microstructure de la pâte de ciment auto-compactante (SCC) contenant comme filler de la poudre calcaire. Sur base d'une série de résultats expérimentaux—par exemple~: tests de calorimétrie par conduction thermométrique isotherme, analyse d'images par microscopie électronique environnementale (ESEM), analyse thermogravimétrique (TGA), analyse thermogravimétrique dérivée (DTG)—, le processus d'hydratation, la distribution de la phase solide, la porosité totale et la distribution de la taille des pores ont été déterminés à différentes étapes de l'hydratation.*

*Sur base de la chimie et de la stoechiométrie de l'hydratation et de la cinétique de l'hydratation du ciment en présence de calcaire, un modèle analytique d'hydratation ainsi qu'un modèle de la microstructure de la pâte de ciment auto-compactante sont proposés. Des simulations concernant deux mélanges de SCC avec un rapport E/C de, respectivement, 0,41 et 0,48 et un rapport eau / poudre*

G. Ye (✉) · K. van Breugel
Microlab, Faculty of Civil Engineering and Geosciences, Delft University of Technology, Delft, The Netherlands
e-mail: ye.guang@citg.tudelft.nl

A. M. Poppe · G. De Schutter · G. Ye
Magnel Laboratory for Concrete Research, Department of Structural Engineering, Ghent University, Ghent, Belgium

X. Liu
School of Civil Engineering, Tongji University, Shanghai, China

*(W/P) de 0,27 ont été menées. Les résultats ont été comparés avec ceux d'une pâte de ciment traditionnelle (TC) dont le rapport E/C vaut 0,48. Les résultats de la simulation ont été discutés et validés en les comparant avec des mesures expérimentales.*

**Keywords** Numerical simulation · Hydration · Microstructure · Self-compacting concrete · Limestone powder

## 1 Introduction

In general, there are two different ways to use limestone powder in construction. One way is the Portland cement blended with limestone powder, so called Portland limestone cement. To produce Portland limestone cement, the limestone is added during the milling of the cement clinker. In the past few years, Portland limestone cement has been accepted worldwide. The ASTM C150 standard specification for Portland cement was modified to allow the incorporation of limestone up to a 5% mass fraction in ordinary Portland cement [1]. In Europe, the European standard EN 197-1 identified two types of Portland limestone cement containing 6–20% lime (type II/A-L) and 21–35% limestone (type II/B-L) [2, 3]. Another way to use limestone filler is to add it during the mixing of Self-Compacting Concrete (SCC) or high performance concrete. The total amount of limestone powder in SCC can reach up to 100% by weight of the cement. The major benefits in using limestone in SCC are both technical and economical. On one hand to ensure high fluidity and to reduce the water/cement ratio, on the other hand to reduce the cost of concrete.

The addition of limestone filler in blended limestone cement was believed to mainly produce a physical effect [4]. However, several authors also reported that limestone filler participates actively in the hydration process of ordinary Portland cement rather than just acting as a mere physical filler [5–8]. As for the influence on the early age hydration of cement, due to the high surface area of limestone powder in the mixtures, it provides sites for the nucleation and growth of hydration products, thus improving the hydration rate of cement compounds and consequently increasing the strength at early age [9–11]. As for the influence on the later stage, from a chemical point of view, limestone filler does not have pozzolanic properties, but it reacts with the alumina phases of cement to form an AFm phase (calcium monocarboaluminate hydrates) with no significant change on the strength of blended cement. On the other hand, limestone filler acts as the crystallization nucleus of the precipitation of CH [12].

Due to the different blending processes and the high amount of limestone filler in SCC, the situation in this case is different compared to Portland limestone cement. It is expected that the hydration behaviour and the microstructure of SCC containing limestone powder as filler also will be different. The influence of limestone in SCC is more related to the physical effects rather than chemical effects [13]. Details on the influence of limestone filler on the hydration and the microstructure are experimentally obtained by means of thermometric isothermal conduction calorimetry, thermogravimetric analysis and derivative thermogravimetric analysis (TGA/DTG), and backscattering scanning electron (BSE) image analysis. A short review is given in the next paragraph. The aim of this paper is, based on the experimental results, to propose a cement hydration microstructural model in order to simulate the hydration and microstructure of SCC. The model is based on HYMOSTRUC3D [14, 15]. Two SCC mixtures with w/c 0.41 and w/c 0.48 and both with water/powder ratio (w/p) 0.27 were simulated and compared to a traditional cement paste (TC) with w/c 0.48. The simulation results were discussed and validated against experimental measurements.

## 2 Review of the experimental results on the hydration and the development of microstructure of SCC in the early age

The hydration and the development of microstructure of SCC were examined and presented in [13, 16]. Experimental results are summarised in the following paragraphs.

### 2.1 Experimental techniques

In the experiments, the hydration process of a series of samples made with varying cement type

and water/powder ratio was studied by means of thermometric isothermal conduction calorimetry (TEM Air 314). To determine the development of the microstructure, only two types of SCC (namely SCC01 and SCC02) were used and compared with a traditional cement paste (TC) with w/c ratio 0.48. The mix proportions used in the experiments are listed in Table 1.

In the experiments, the distribution of the phase (the capillary pore, CSH gel, CH, limestone filler and unhydrated cement) was identified by using BackScattering Electron (BSE) microscopy image analysis. In order to obtain high quality images from the BSE detector, the samples were prepared carefully, this including epoxy impregnation, cutting, grinding (on the middle-speed lap wheel with p320, p500 and p1200 sand papers) and polishing (on a lap wheel with 6, 3, 1, and 0.25 μm diamond pastes for about 2 min each). The images are obtained using a BSE detector in water vapour mode. In order to get a high contrast image for image analysis, a low acceleration voltage of about 20 kV was used. The physical size of the region in each image is 263μm in length and 186μm in width when a magnification of 500 × is used. The image size is 1,728 × 1,027 pixels, so the resolution is 0.152 μm per pixel. The results calculated on the average value of 10 samples at different curing age.

Thermal investigation by means of thermogravimetric analysis and derivative thermogravimetric analysis were done to quantitatively calculate the weight loss of each individual phase at atmospheric pressure, in nitrogen (TA Instruments 2960 SDT V3.0F, 10°C/min, up to 1,200°C). About 30 mg of each sample at the age of 28 days was tested.

**Table 1** Mix proportions of the cement paste (kg/m$^3$)

| | TC | SCC01 | SCC02 |
|---|---|---|---|
| Portland cement I 52.5 | 350 | 400 | 400 |
| Water | 165 | 165 | 192 |
| Limestone powder | | 200 | 300 |
| Glenium 51 (liter/m$^3$) | | 3.2 | 2.7 |
| Total powder content | 350 | 600 | 700 |
| Water/powder ratio | 0.48 | 0.27 | 0.27 |
| Water/cement ratio | 0.48 | 0.41 | 0.48 |

## 2.2 Summary of experimental results

### *2.2.1 Heat release*

From fig. 1a, it can be concluded that the samples of SCC made with limestone filler (SCC01 and SCC02) show a higher heat release than traditional cement paste, especially in the first 24 h. The mixtures made with limestone filler show a shorter dormant stage and a more rapid heat release than mixtures without limestone filler. An extremum was found for both SCC mixtures at 12 h. The rate of heat release curve (Fig. 1b) also indicates the rapid chemical reaction of SCC in the early stage. For a detailed discussion on the heat release and hydration of SCC reference is made to [16, 17].

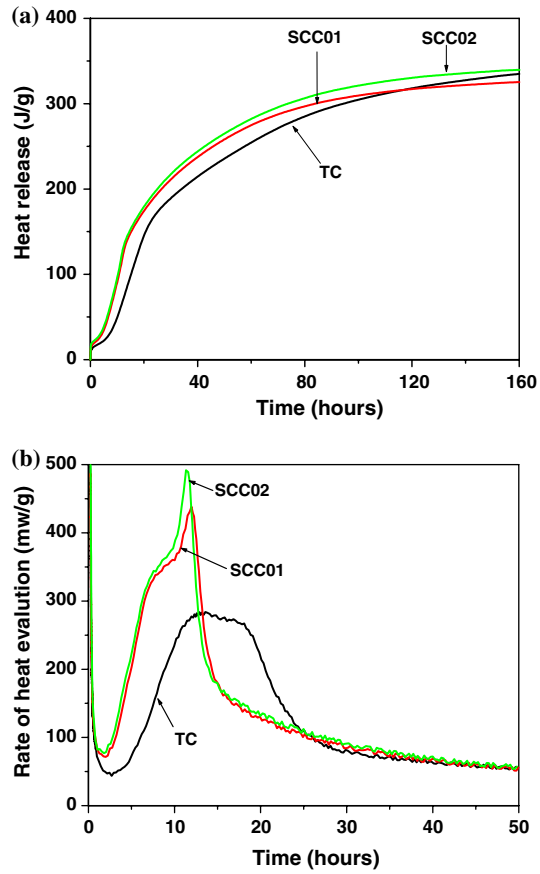


**Fig. 1** (**a**) Heat release of 3 different mixtures at 20°C in the first 200 h and (**b**) The rate of heat release of 3 different mixtures in the first 50 h at 20°C

To explain these phenomena two divergent hypotheses can be followed. The first hypothesis states that the limestone filler is inert and therefore does not take part in the reactions during the hydration. On the one hand, it will figure as a nucleation core for the hydration of the $C_3S$ and $C_2S$ and shorten the dormant stage and fasten the hydration reactions. On the other hand the filler will activate reactions that are not or less prominently present in a traditional concrete without limestone filler which results in the third peak in the curve of the heat production rate.

The second hypothesis does not consider the limestone filler to be inert, but sees it as an active partner in the hydration reactions. The appearance of the extra hydration peak might then be explained by a conversion of ettringite to monocarbonate instead of monosulphate, which is a more stable compound and therefore results into more heat release, this with a peak at about 12 h after the mixing of the components as a result.

### 2.2.2 *Thermal analysis*

Results on the thermal decomposition of 3 cement pastes at curing age 28 days are shown in Fig. 2. Details on the interpretation of TGA/DTG results of SCC were reported elsewhere [13], only the decomposition of limestone powder is mentioned hereafter.

Around 750°C, an extremum was found from DTG (Fig. 2b). Correspondingly, a dramatic loss of mass was also observed from TGA (Fig. 2a), representing the decomposition of carboniferous, $CaCO_3 \rightarrow CaO + CO_2$, with $CO_2$ escaping.

The amount of $CO_2$ escaping from cement paste can be calculated exactly from the TGA tests and compared with theoretical calculations. From fig. 2a, a mass loss of 10.29% and 13.25% can be calculated for SCC01 and SCC02, respectively. If the total weight of the SCC01 and SCC02 sample was 28.9948 mg and 28.5063 mg, then the total amount of $CO_2$ escaping from the TG analysis is 2.78 mg and 3.78 mg, respectively. Theoretically, according to the weight percentage of limestone filler in the mixture, there is 7.54 mg and 9.56 mg $CaCO_3$ present in the sample of SCC01 (28.9948 mg) and SCC02 (28.5063 mg).

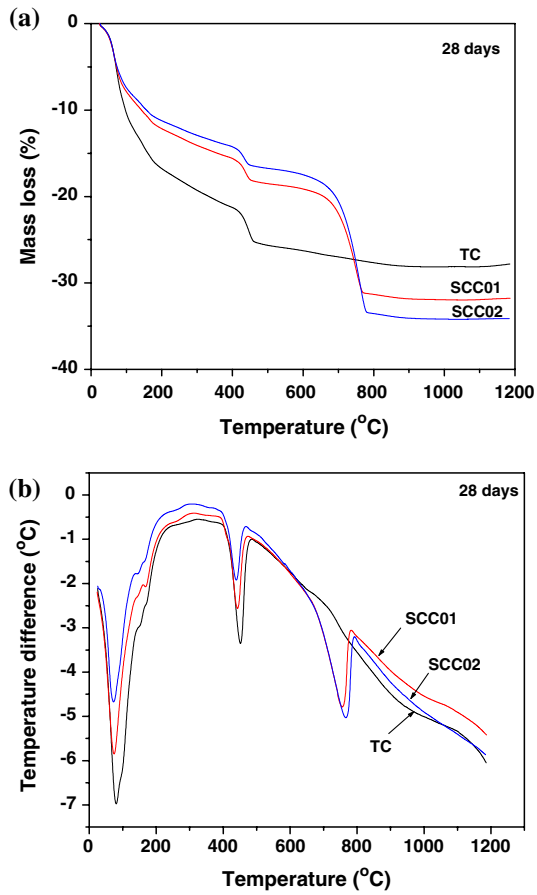


**Fig. 2** (**a**) The thermal decomposition of the cement paste by the thermogravimetric analysis (TGA) and (**b**) the derivative thermogravimetric analysis (DTG) of three samples

The amount of $CO_2$ escaping from decomposition of carboniferous, $CaCO_3 \rightarrow CaO + CO_2$, should be 2.86 mg for SCC01 and 3.63 mg for SCC02.

Comparing the TGA analysis and the theoretical calculations, the weight loss from the TGA analysis is slightly bigger than the weight loss from the theoretical calculations. If one takes into account a small part of the weight loss is due to the decomposition of the calcium silicate hydrates in the cement paste, the main part of the weight loss at this temperature is due to decarbonation of the limestone. According to the mass balance law, it can be found that almost no limestone powder participated in the chemical reaction during cement hydration. The limestone powder acts only as inert filler in the SCC.

### 2.2.3 BSE image analysis

The backscattering electron images from samples SCC02 and TC at the age of 7 days are shown in fig. 3. From image analysis it is found that the interface between limestone and hydrates is quite porous. The evolution of total porosity and $CaCO_3$ is shown in fig. 4. It can be found that the amount of $CaCO_3$ almost did not change during the 28 days of hydration. This also agrees with the results observed by TGA.

From experimental results discussed above, the following conclusions can be made

1. The presence of limestone powder in SCC promotes the chemical reaction and thus increases the hydration rate at early stage. This agrees with the conclusion made by other investigators [8–11].
2. The mass of limestone powder does not change even at the hydration age of 28 days. Limestone powder can be treated as inert in the mixtures at the micro level.

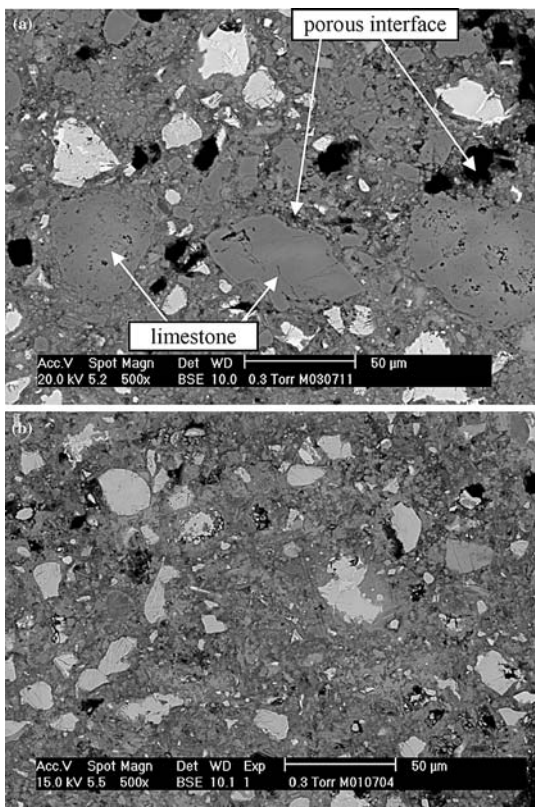


**Fig. 3** Comparison of BSE images for SCC02 (**a**) and TC (**b**) at age of 7 days

## 3 Modelling of SCC

### 3.1 Analytical hydration model

According to a series of isothermal hydration tests, the heat production rate of a Portland cement $q$ at certain temperature ($\theta$) can be calculated as follows [15]:

$$q = q_{\max,20} \cdot f(r) \cdot \exp\left[\frac{E}{R}\left(\frac{1}{293} - \frac{1}{273+\theta}\right)\right] \quad (1)$$

where, $q_{\max,20}$ is the maximum heat production rate at 20°C, $E$ is the apparent activation energy

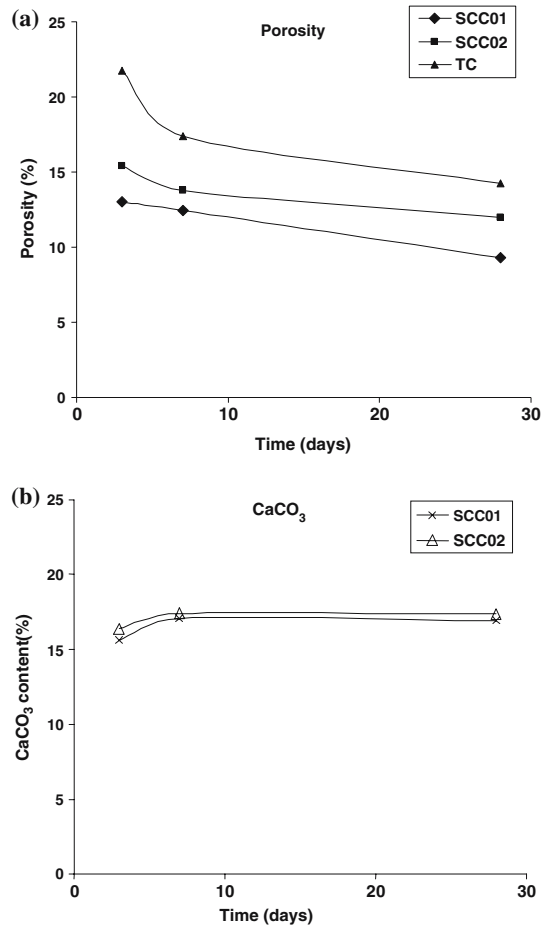


**Fig. 4** The evolution of total porosity and $CaCO_3$

and $R$ is the universal gas constant. The function $f(r)$ can be calculated as:

$$f(r) = \mathrm{c} \cdot [\sin(r\pi)]^{\mathrm{a}} \cdot \exp(-\mathrm{br}) \tag{2}$$

where, $a$, $b$ and $c$ are the parameters

When looking into the results of the isothermal tests, it can be clearly seen that the hydration mechanism of SCC with limestone filler cannot be described as one function as done for a traditional concrete with Portland cement. The presence of the limestone filler makes a second reaction appear, which has to be modelled separately. The superposition principle is then applied in order to obtain the total cement reaction.

### 3.1.1 First reaction

When applying the model as for traditional concrete to the first reaction of the SCC hydration, the parameters calculated by the least squares method seem to be influenced by the addition of the filler and can be modelled as a second degree function of the c/p factor. The first hydration reaction can be described mathematically as follows [15]:

$$q_1 = q_{1,\max,20} \cdot c_1 \cdot [\sin(r_1\pi)]^{a_1} \cdot \exp(-3r_1) \times \exp\left[\frac{E_1}{R}\left(\frac{1}{293} - \frac{1}{273+\theta}\right)\right] \tag{3}$$

$$a_1 = -0.18(c/p)^2 + \gamma_1(c/p) + \gamma_0 \tag{4}$$

$$c_1 = -0.28(c/p)^2 + \beta_1(c/p) + \beta_0 \tag{5}$$

With $q_{1,\max,20}$, the maximum heat production rate at 20°C of the first reaction, $E_1$ the apparent activation energy of the first reaction and $a_1$ and $c_1$, the parameters.

### 3.1.2 Second reaction

The second reaction activated by the presence of the limestone filler can be described as

$$q_2 = q_{2,\max,20} \cdot [\sin(r_2\pi)]^{a_2} \cdot \exp\left[\frac{E_2}{R}\left(\frac{1}{293} - \frac{1}{273+\theta}\right)\right] \tag{6}$$

With $q_{2,\ \max,20}$, the maximum heat production rate at 20°C of the second reaction, $E_2$ the apparent activation energy of the second reaction and $a_2$ and $c_2$, the parameters.

As can be seen in fig. 1, the second reaction does not start immediately after water addition. It is not clear yet why this is happening. Further tests are done with the aim to investigate the nature of the second reaction, and how and at which moment during hydration it is activated.

### 3.1.3 Degree of hydration

Once the heat production rate is determined, the degree of reaction can be determined as a function of time. To do so the superposition principle and discrete integration is used, which results in :

$$r(t+\mathrm{d}t) = \frac{Q_{1\max}}{Q_{\max}} \cdot \left(r_1(t) + \frac{q_{1\max,20} \cdot g_1(\theta) \cdot f_1(r_1) \cdot \mathrm{d}t}{Q_{1\max}}\right) + \frac{Q_{2\max}}{Q_{\max}} \cdot \left(r_2(t) + \frac{q_{2\max,20} \cdot g_2(\theta) \cdot f_2(r_2) \cdot \mathrm{d}t}{Q_{2\max}}\right) \tag{7}$$

After the calculation of the degree of reaction it is fairly easy to make the step to degree of hydration, since it is established experimentally that the formula of Mill for the ultimate degree of hydration is still applicable for self-compacting concrete. This means that the degree of hydration can be calculated as :

$$\alpha(t) = \alpha_u \cdot r(t) \tag{8}$$

with $\alpha_u = \frac{1.031 \cdot w/c}{0.194 + w/c}$ = the ultimate degree of hydration.

## 3.2 Microstructural modelling

Simulation of the development of the microstructure of SCC containing limestone filler is based on the 3D cement hydration computer model HYMOSTRUC3D [14, 15]. In the original HYMOSTRUC model [14], only cement particles were considered. In order to simulate the hydration of cement containing limestone powder, the characteristics of the paste have to be modified.

For a fully description of the original HYMOSTRUC model, see [14].

### 3.2.1 Particle size distribution of cement and limestone powder

The cumulative particle size distribution of the cement and limestone powder is described using the Rosin–Rammler function:

$$G_{\mathrm{cem}}(x) = 1 - \exp(-b_{\mathrm{cem}} \times x^{n_{\mathrm{cem}}}) \tag{9}$$

$$G_{\mathrm{lim}}(x) = 1 - \exp(-b_{\mathrm{lim}} \times x^{n_{\mathrm{lim}}}) \tag{10}$$

where, $G_{\mathrm{cem}}(x)$, $G_{\mathrm{lim}}(x)$ are the under-size of particles $< x$ μm for cement particles and limestone particles, respectively. $b_{\mathrm{cem}}$, $n_{\mathrm{cem}}$, $b_{\mathrm{lim}}$ and $n_{\mathrm{lim}}$ are Rosin–Rammler constants.

The cement mass $W_{\mathrm{cem}}(x)$ of the fraction $F_{\mathrm{cem}}(x)$ and the limestone powder mass $W_{\mathrm{lim}}(x)$ of the fraction $F_{\mathrm{lim}}(x)$ are obtained by differentiating Eq. 9 and Eq. 10 with respect to $x$:

$$W_{\mathrm{cem}}(x) = \gamma \times b_{\mathrm{cem}} \times n_{\mathrm{cem}} \times x^{n_{\mathrm{cem}}-1} \times \mathrm{e}^{-b_{\mathrm{cem}} x^{n_{\mathrm{cem}}}} \tag{11}$$

$$W_{\mathrm{lim}}(x) = \gamma \times b_{\mathrm{lim}} \times n_{\mathrm{lim}} \times x^{n_{\mathrm{lim}}-1} \times \mathrm{e}^{-b_{\mathrm{lim}} x^{n_{\mathrm{lim}}}} \tag{12}$$

where, $\gamma$ is a constant [14].

For the volume $V_{\mathrm{cem}}(x)$ and $V_{\mathrm{lim}}(x)$ of all particles in fraction $F_{\mathrm{cem}}(x)$ and $F_{\mathrm{lime}}(x)$ it holds that:

$$V_{\mathrm{cem}(x)} = \frac{W_{\mathrm{cem}}(x)}{\rho_{\mathrm{cem}}} \tag{13}$$

$$V_{\mathrm{lim}(x)} = \frac{W_{\mathrm{lim}}(x)}{\rho_{\mathrm{lim}}} \tag{14}$$

The number of particles $N_{\mathrm{cem}}(x)$ and $N_{\mathrm{lim}}(x)$ in fraction $F_{\mathrm{cem}}(x)$ and $F_{\mathrm{lim}}(x)$ are found by dividing the volume $V_{\mathrm{cem}}(x)$ and $V_{\mathrm{lim}}(x)$ of fraction $F_{\mathrm{cem}}(x)$ and $F_{\mathrm{lim}}(x)$ by the volume of a single particles $v_{\mathrm{cem}}(x)$ and $v_{\mathrm{lime}}(x)$

$$N_{\mathrm{cem}(x)} = \frac{V_{\mathrm{cem}(x)}}{v_{\mathrm{cem}(x)}} \tag{15}$$

$$N_{\mathrm{lim}(x)} = \frac{V_{\mathrm{lim}(x)}}{v_{\mathrm{lim}(x)}} \tag{16}$$

### 3.2.2 Paste characteristics

The specific mass $\rho_{\mathrm{pa}}$ of a paste containing limestone powder with a w/c=$\omega_0$ can be expressed as follows:

$$\rho_{\mathrm{pa}} = \frac{1 + \omega_0 \times \left(\frac{1}{P}\right) + \left(\frac{1-P}{P}\right)}{\rho_{\mathrm{w}}\rho_{\mathrm{lim}} + \rho_{\mathrm{w}}\rho_{\mathrm{lim}}\omega_0\left(\frac{1}{P}\right) + \rho_{\mathrm{cem}}\rho_{\mathrm{w}}\left(\frac{1-P}{P}\right)} \tag{17}$$

where $P$ is the mass ratio of cement and limestone powder. $\rho_{\mathrm{cem}}$, $\rho_{\mathrm{lim}}$, $\rho_{\mathrm{w}}$ are the density of cement, limestone powder and water, respectively.

In the original HYMOSTRUC model [14], a cell $I_x^c$ is defined as a cubic space in which the largest cement particles has a diameter x, and the further consists of $1/N_{x;\mathrm{cem}}$ times the original water volume and of $1/N_{x;cem}$ times the volume of all particles with diameter smaller than that of particles $x$. When the model incorporates limestone powder, the cell definition is rewritten as:

$$I_x^c = \frac{\omega_0 + (1 - m_{\mathrm{lim}})\frac{G_{\mathrm{cem}}(x)}{\rho_{\mathrm{cem}}} + m_{\mathrm{lim}}\frac{G_{\mathrm{lim}}(x)}{\rho_{\mathrm{lim}}}}{N_{x;\mathrm{cem}}} \tag{18}$$

The volumetric cell density for cement is:

$$\zeta_x^{\mathrm{cem}} = \frac{1 - m_{\mathrm{lim}}}{(1 - m_{\mathrm{lim}}) + \omega_0\frac{\rho_{\mathrm{cem}}}{G_{\mathrm{cem}}(x)} + m_{\mathrm{lim}}\frac{G_{\mathrm{lim}}(x)}{G_{\mathrm{cem}}}\frac{\rho_{\mathrm{cem}}}{\rho_{\mathrm{lim}}}} \tag{19}$$

The shell density for cement is

$$\zeta_{\mathrm{sh;s,d_u}} = \frac{\zeta_x^{\mathrm{cem}} \times I_x^c - v_{x;\mathrm{cem}}}{I_x^c - v_{x;\mathrm{cem}}} \tag{20}$$

### 3.2.3 Particle growth, interaction mechanisms

The volume of the outer product $V_{\mathrm{ou};x}^{\mathrm{cem}}$ for the cement particles at a degree of hydration $\alpha$ can be described as:

$$V_{\mathrm{ou};x}^{\mathrm{cem}} = (v^{\mathrm{cem}} - 1)\alpha \times V_x^{\mathrm{cem}} \tag{21}$$

Similarly, the volume of the outer product for the limestone powder $V_{ou;x}^{\mathrm{lim}}$ can be described as

$$V_{\mathrm{ou};x}^{\mathrm{lim}} = \left(v^{\mathrm{lim}} - 1\right)\alpha \times V_x^{\mathrm{lim}} \tag{22}$$

where, $\alpha$ is overall degree of hydration according to Eq. 8. $v^{cem}$ is the volume ratio of the reaction product and the dissolved material of cement as described in [14], $v^{lim}$ is the volume ratio of the reaction product and the dissolved material of limestone powder. These two parameters directly control the reaction ratio of cement and fillers. In the case of limestone powder acting only as inert filler without participating in the chemical reactions, the $v^{lim}$ should be equal to 1. Thus, there are no outer products formed around the limestone particles.

Once the volume of outer products has been determined, the radius of the expanding central cement particle and the volume of expanded outer shell can be deduced according to [14].

## 4 Results and discussions

Simulation of the hydration process and the microstructure of SCC containing limestone filler starts from the cement and limestone particle size distribution. The minimum particle size of the limestone and cement was 0.5 μm and the interval of the particle size was 0.5 μm. The Blaine specific surface area of cement and limestone powder are 526 $m^2$/kg and 420 $m^2$/kg, respectively. In fig. 5, the simulated particle size distribution of cement and limestone agrees quite well with the experiments measured by the Low Angle Laser Light Scattering (LALLS) method. The input of the

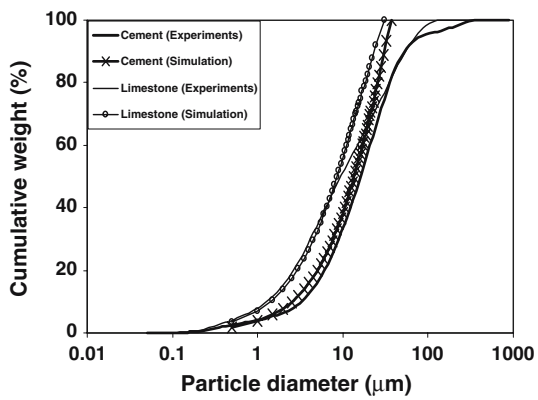


**Fig. 5** Simulated PSD of cement and limestone powder compared with experiments

**Table 2** The chemical composition of cement

| | CEM I 52.5 (%) |
|---|---|
| CaO | 63.95 |
| $SiO_2$ | 20.29 |
| $Al_2O_3$ | 4.52 |
| $Fe_2O_3$ | 2.35 |
| MgO | 2.22 |
| $K_2O$ | 0.94 |
| $Na_2O$ | 0.20 |
| $SO_3$ | 3.35 |
| $Cl^-$ | 0.015 |

**Table 3** The amount of cement and limestone particles distributed in 100 $\mu m^3$ cube

| | Cement particles | Limestone powder |
|---|---|---|
| TC | 147189 | – |
| SCC01 | 125868 | 160721 |
| SCC02 | 106114 | 207765 |

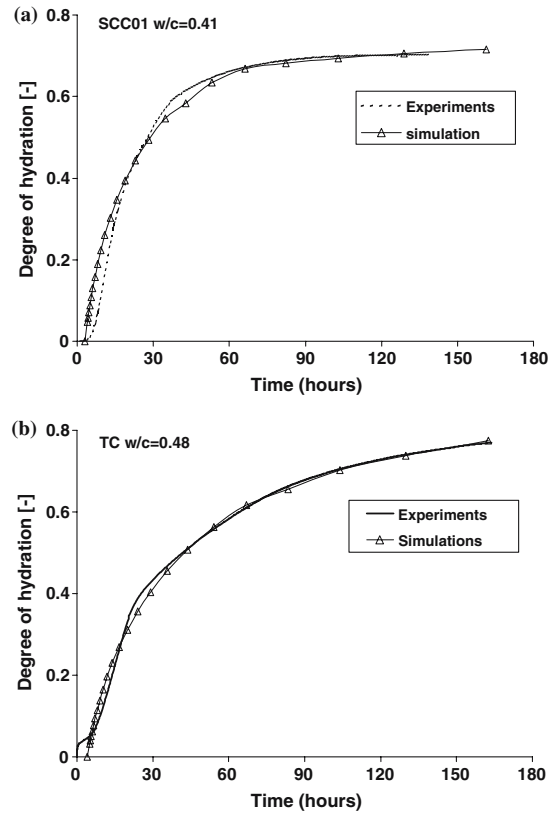


**Fig. 6** Comparison of degree of hydration from experiments and from computer simulation model for the samples SCC01 (**a**) and TC (**b**)

chemical composition of the cement used in the simulation is listed in Table 2.

The simulated cubic body of paste was 100 $\mu m^3$. The total amount of distributed cement particles and limestone particles in the cube are listed in Table 3. According to Eq. 22, the limestone powder does not expand throughout the hydration process.

Figure 6 shows the degree of hydration of samples SCC01 and TC, on the one hand as calculated from experiments on SCC containing limestone powder, and on the other hand from the computer simulation model. A good agreement is found between experiments and simulations.

The simulated 3D microstructure of SCC02 and TC at the initial stage are shown in Fig. 7a, b. The white particles are limestone powder and the others are cement particles.

Using the algorithm developed by [15], the capillary porosity was calculated from the simulated cement paste at different hydration stages. The results of capillary porosity from the simulations and from the SEM image analysis are illustrated in Fig. 8. Despite the variation of experiments, a good agreement is found between the simulation model and the results obtained by SEM image analysis.

Figure 9 show the 2D simulated microstructure at a hydration stage $\alpha = 0.62$. The particles with dark grey colour are limestone powder particles. The calculated porosity of SCC02 and TC at this hydration stage is 10% and 17.4%, respectively. From Table 3, the total amount of particles in SCC02 is more than 300,000, 2 times higher than in TC. In principle, due to the addition of limestone as inert filler in the SCC, the porosity of SCC is much lower than of TC even having the same w/c ratio. From Fig. 9, it is noted that limestone powder fills up the empty pores. However, the porosity around the limestone filler particles also is much bigger than the porosity around the hydrated cement particles. This is

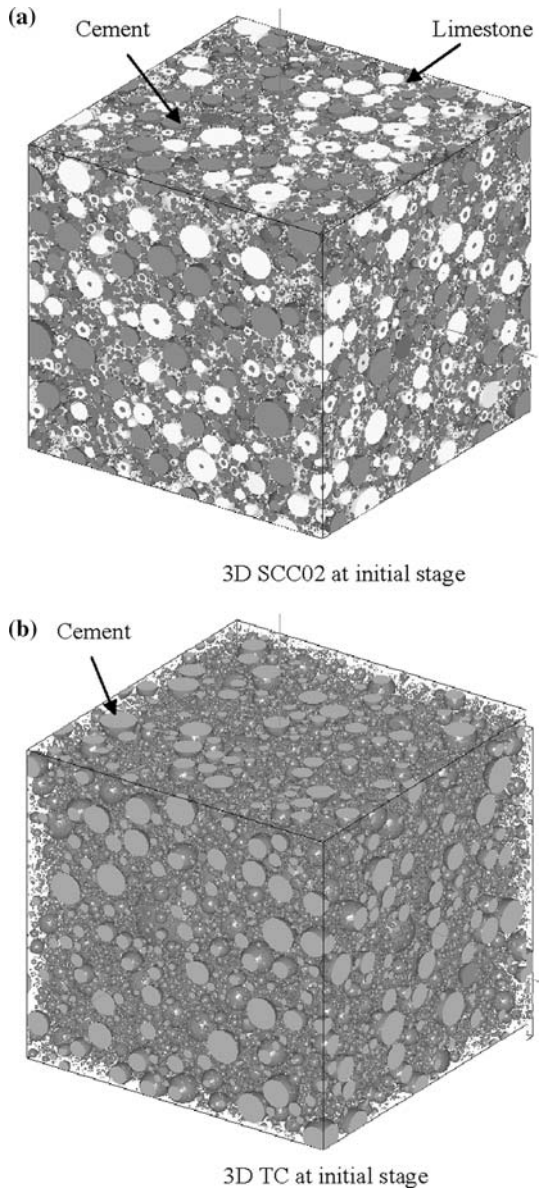


**Fig. 7** 3D simulated microstructure of SCC02 (**a**) and TC (**b**) at initial stage

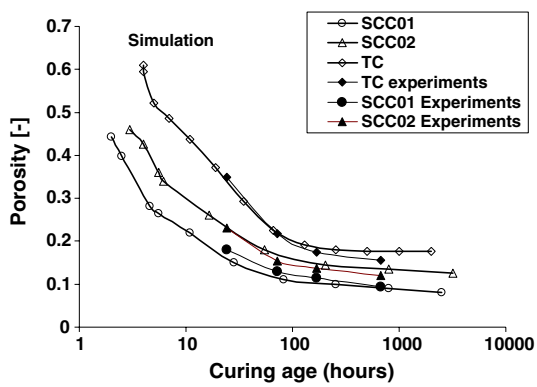


**Fig. 8** Comparison of capillary porosity from computer simulation model of SCC and experiments from BSE analysis

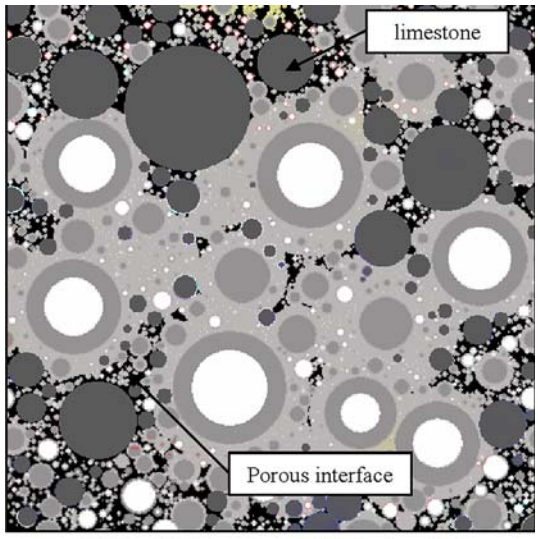


(a) 2D SCC02 at degree of hydration 0.62

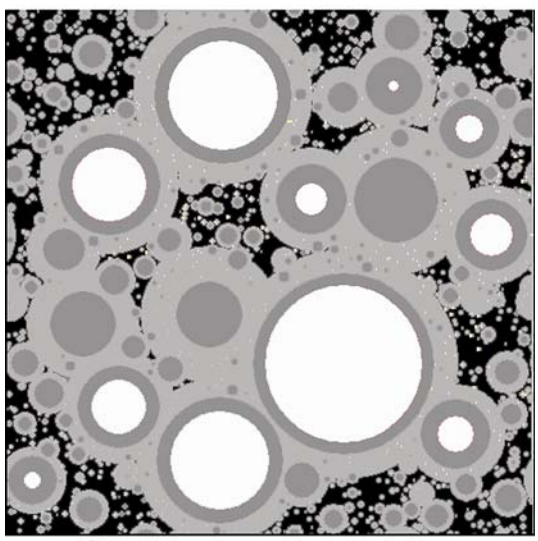

(b) 2D TC at degree of hydration 0.62

**Fig. 9** (**a**) 2D structure of SCC02 at a degree of hydration of 0.62, porosity 10.0% (**b**) 2D structure of TC at a degree of hydration of 0.62, porosity 17.4%

consistent with the experiments where the interface between limestone filler and hydrates is quite porous, even on the samples at the age of 28 days [13].

## 5 Conclusions

HYMOSTRUC3D cement hydration computer model has been modified to simulate the self-compacting cement paste containing limestone powder as filler. The hydration process and the microstructure of SCC investigated by heat release, TGA/DTG and BSE imaging technique were reviewed. The chemical effects of limestone powder were considered in the hydration models by taking into account the secondary chemical reaction. The fine filler effect of limestone powder was simulated in the microstructure mode. Two SCC paste samples were simulated and the pore structure was analysed and compared with the traditional concrete. The evolution of porosity simulated from the model agrees well with the experiments from the BSE image analysis. Further research will be focusing on the percolation of capillary porosity of SCC and the development of strength influenced by limestone powder.

## References

1. ASTM Annual Book of Standards, Vol. 04.01 Cement; Lime; Gypsum, American Society for Testing and Materials, West Conshohocken, PA, 2004
2. Dhir R, Jones M (1994) Euro-cements. Impact of ENV 197-1 on concrete construction. London, Eand FN Spon
3. European Committee for Standardization. (2000) EN 197–1
4. Vuk T, Tinta V, Gabrovšek R, Kaučič V (2001) The effects of limestone addition, clinker type and fineness on properties of Portland cement. Cement Concrete Res 31(1):135–139
5. Péra J, Husson S, Guilhot B (1999) Influence of finely round limestone on cement hydration. Cement Concrete compose 21(2):99–105
6. Tsivilis S, Chaniotakis E, Badogiannis E, Pahoulas G (Thens 1996) 'Strength development of Portland limestone cements, in Proceedings of 16th Hellenic Conference on Chemistry 555–8
7. Soroka I, Sterm N (1997) The effect of fillers on strength of cement mortars. Cement Concrete Res 7(4):449–456
8. Gutteridge W, Dalziel J (1990) Filler cement. The effect of the secondary component on the hydration of Portland cement: part 1. A fine non-hydraulic filler. Cement Concrete Res 20(5):778–782
9. Bonavetti V, Donza H, Rahhal VF, Irassar EF (2000) Effect of initial curing on properties of concrete with limestone filler cement. Cement Concrete Res 30(5):703–708
10. Heikal M, EL-Didamony E, Morsy MS (2000) Limestone-filled pozzolanic cement. Cement Concrete Res 30:1827–1834

11. Xiong X, van Breugel K (Cairo, 2003)Effect of limestone powder and temperature on cement hydration processes. In: EI-Dieb AS, Reda Taha MM, Lissel SL (eds), International conference on performance of construction materials in the new millennium (2)231–241
12. Bentz DP (2005) Modeling the influence of limestone filler on cement hydration using CEMHYD3D. Cement Concrete compose 28(2):124–129
13. Ye G, Liu X, De Schutter D, Poppe A-M, Taerwe L (2005) Hydration and microstructure studies on self-compacting cement paste containing limestone powder as filler. Cement Concrete Compose (accepted)
14. van Breugel K (1991) Simulation of Hydration and Formation of Structure in Hardening Cement-Based Materials. PhD Thesis, Delft University of Technology, The Netherlands
15. Ye G (2003) Experimental study and numerical simulation of the development of the microstructure and permeability of cementitious materials. PhD Thesis, Delft university of technology, The Netherlands
16. Poppe A-M (2004) Influence of fillers on hydration and properties of self-compacting concrete. PhD Thesis (in Dutch), Ghent University
17. De Schutter G (1996). Fundamental and practical study of thermal stress in hardening massive concrete elements. PhD Thesis (in Dutch), Ghent University